Romé et al., http://www.jcb.org/cgi/content/full/jcb.201001144/DC1

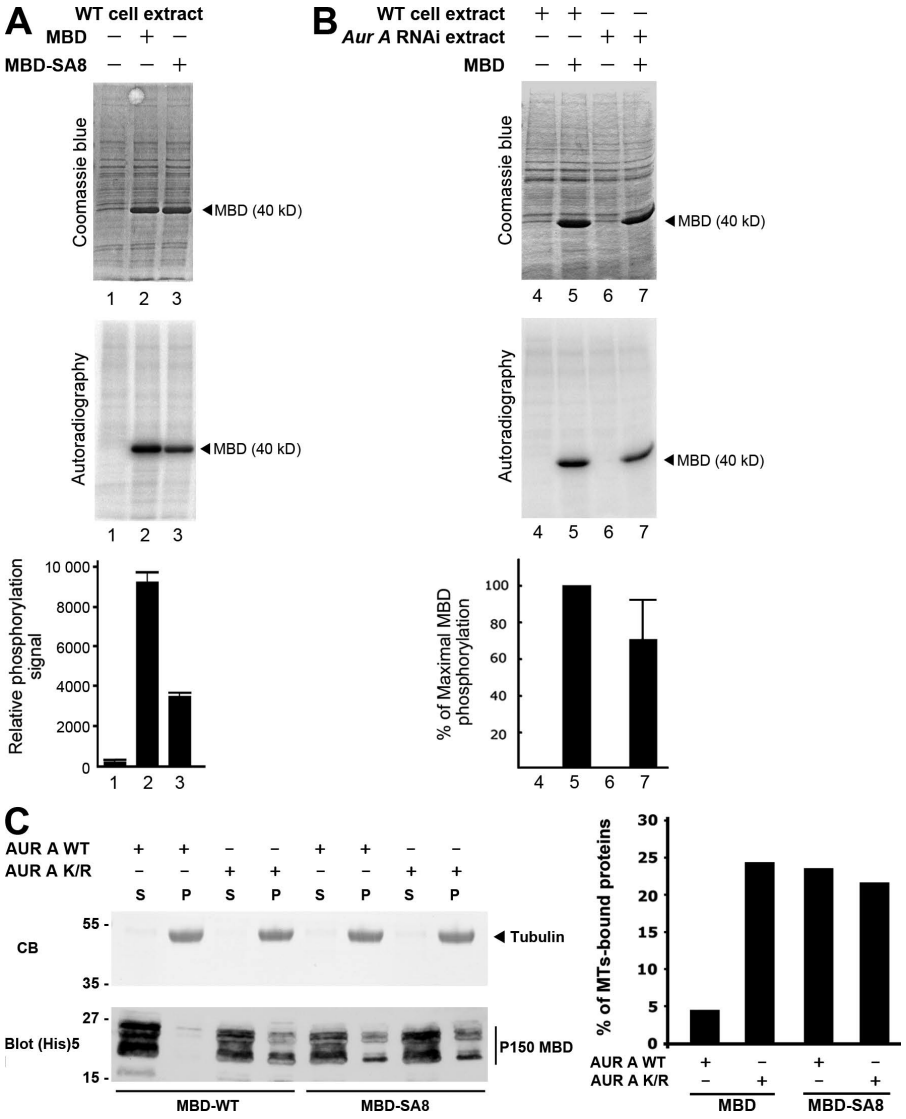

Figure S1. **Analysis of p150^{glued} MBD phosphorylation in vivo and effect on microtubule binding in vitro.** (A) p150^{glued} MBD (lane 2) or MBD-SA8 (lane 3) were phosphorylated by wild-type (WT) S2 cell extracts. Note the strong decrease of MBD-SA8 phosphorylation compared with MBD, indicating that identified aurora A phosphorylation sites correspond to ∼60% of the overall in vivo phosphorylation of this fragment (n = 5; compare lane 2 with lane 3). (B) Wild-type (lanes 4 and 5) or aurora A–depleted cell extracts (lanes 6 and 7) were used to phosphorylate wild-type MBD (lanes 5 and 7). After aurora A depletion (compare lane 5 with lane 7), MBD phosphorylation decreases by ∼25% (n = 6). (C, left) Wild-type MBD or nonphosphorylatable MBD mutant (MBD-SA8) was incubated in the presence of ATP with active (AurA WT) or inactive (AurA K/R) aurora A kinase. The reaction product was incubated with taxol-stabilized microtubules (see Materials and methods) and sedimented at 100,000 g. The microtubule pellets (P) and the supernatants (S) were analyzed by Coomassie blue (CB) staining to reveal tubulins (top) or anti-pentahistidine Western blotting to reveal wild-type MBD or MBD-SA8 (bottom). The arrowhead indicates the position of tubulin (microtubules) in the pellet. In the presence of aurora A K/R, a fraction of wild-type MBD and MBD-SA8 is bound to microtubules. In contrast, in the presence of wild-type aurora A, wild-type MBD cannot bind to microtubules, whereas the MBD-SA8 still does. Thus, specific phosphorylation of MBD by aurora A prevents dynactin binding to microtubules. (C, right) Percentage of total MBD and MBD-SA8 proteins detected in the microtubule pellets. p150^{glued} MBD behavior in this assay was identical in three different experiments. Error bars indicate mean ± SD.

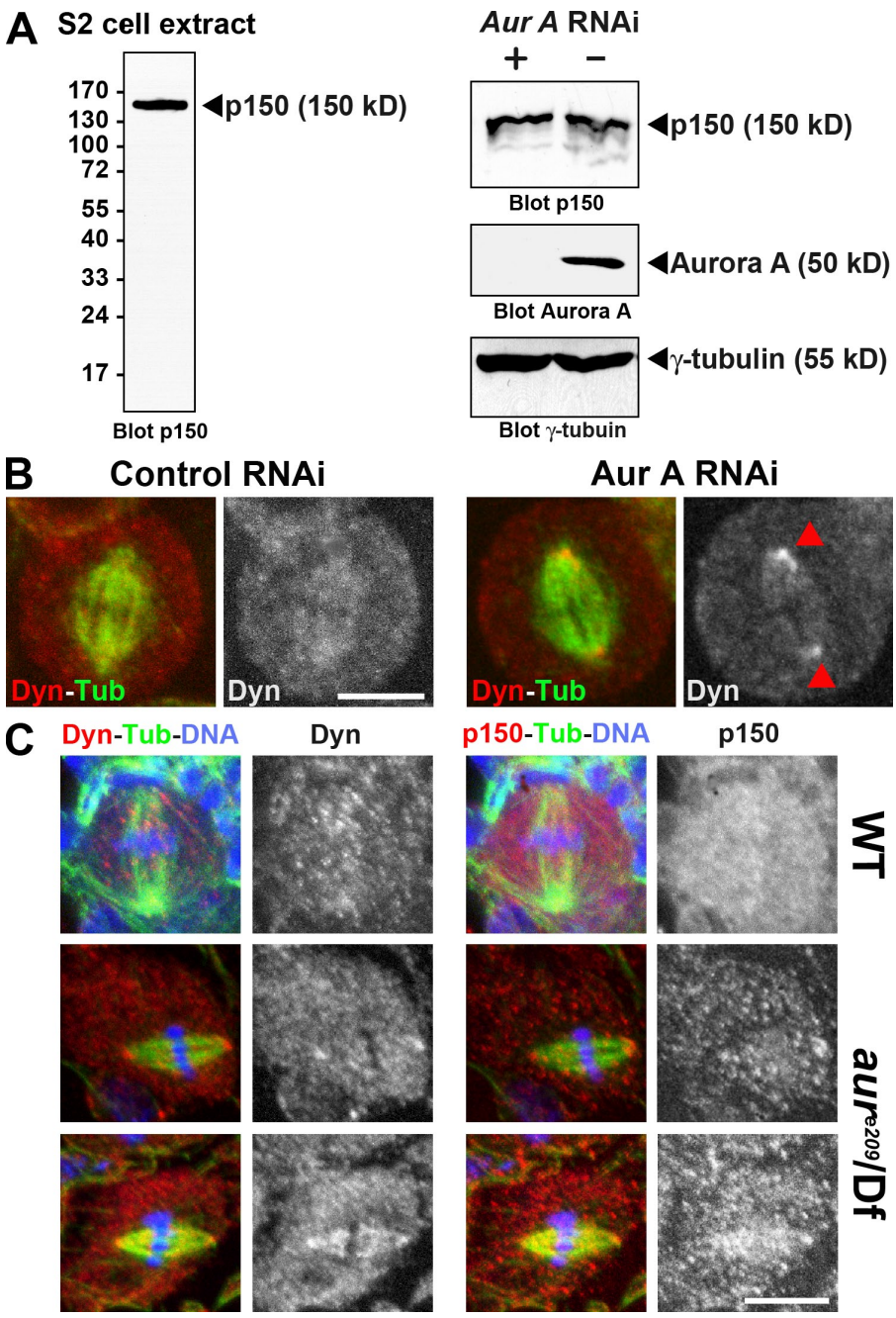

Figure S2. **Analysis of p150^{glued} protein levels in S2 cells, dynein localization in aurora A–depleted S2 cells, and *aurora A* mutant neuroblasts.** (A, right) Western blot of S2 cell extract probed with affinity-purified anti-p150^{glued} antibody. Western blot showing aurora A (middle), γ-tubulin (bottom), or p150^{glued} (top) protein levels in control (−) or *aurora A* RNAi-treated cells (+). Note the strong depletion of the aurora A protein, whereas the p150^{glued} protein levels are unaffected. (B) Control (left) or *aurora A* RNAi-treated S2 cells were stained for tubulin (green) and dynein (red; right in monochrome). Note the accumulation of dynein at spindle poles in *aurora A* dsRNA-treated cells (right, arrowheads). Bar, 5 µm. (C) Wild-type (WT; top) or *aurora A*^{e209}/Df(3R)T61 neuroblasts (bottom) during metaphase were fixed and stained for tubulin (green) and DNA (blue). Note that left and right panels show the same cells stained for p150^{glued} (red; monochrome in left) and dynein (red; monochrome in right). Dynein and dynactin show similar localization patterns in these cells, suggesting that they remain associated in the mutant. Bar, 10 µm.

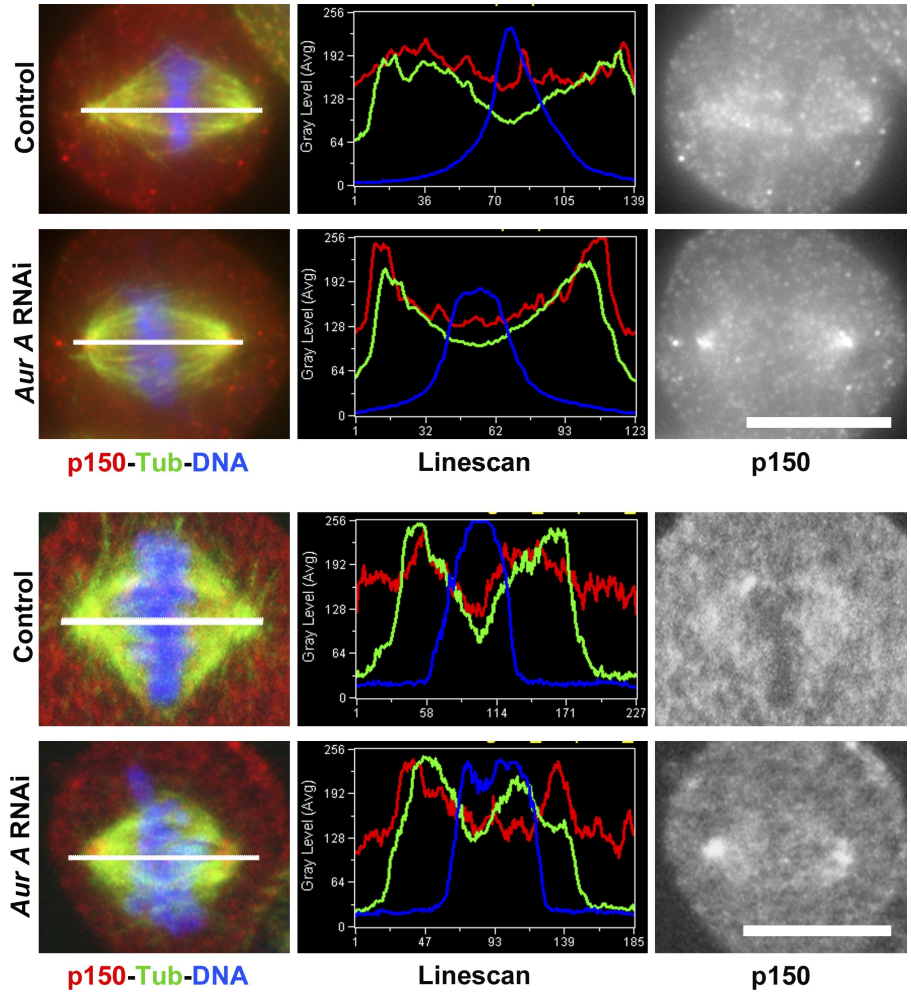

Figure S3. **Distribution of p150^{glued} on the mitotic spindle.** Control or *aurora A* dsRNA-treated cells were stained for microtubules (green), DNA (blue), and p150^{glued} (red). A line scan between the poles was performed to show the relative fluorescence intensity of each fluorophore. Note the strong accumulation of p150^{glued} at the spindle poles of *aurora A* dsRNA-treated cells (compare red line with green line). Bar, 10 µm. The two top panels were acquired with a conventional microscope equipped with a camera. The two bottom cells were also shown in Fig. 5 A (control and aurora A–depleted metaphases).

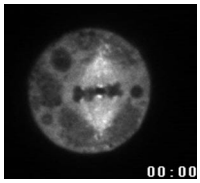

Video 1. **Dynamics of p150-GFP protein in a *Drosophila* S2 cell.** The time (min:s) is displayed at the bottom of the picture.

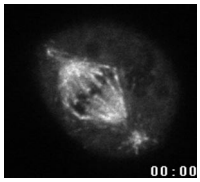

Video 2. **Dynamics of p150-SA8-GFP protein in a *Drosophila* S2 cell.** The time (min:s) is displayed at the bottom of the picture.